Particle detection through the quantum counter concept in YAG:Er3+

A. F. Borghesani, C. Braggio, G. Carugno, F. Chiossi, A. Di Lieto, M. Guarise, G. Ruoso, and M. Tonelli

Citation: Applied Physics Letters **107**, 193501 (2015); doi: 10.1063/1.4935151
View online: http://dx.doi.org/10.1063/1.4935151
View Table of Contents: http://scitation.aip.org/content/aip/journal/apl/107/19?ver=pdfcov
Published by the AIP Publishing

Particle detection through the quantum counter concept in YAG:Er^{3+}

A. F. Borghesani,[1] C. Braggio,[2,a)] G. Carugno,[2] F. Chiossi,[2] A. Di Lieto,[3] M. Guarise,[2] G. Ruoso,[4] and M. Tonelli[3]
[1]*CNISM Unit, Dip. di Fisica e Astronomia and INFN, Via F. Marzolo 8, I-35131 Padova, Italy*
[2]*Dip. di Fisica e Astronomia and INFN, Via F. Marzolo 8, I-35131 Padova, Italy*
[3]*Dip. di Fisica and INFN, Largo Bruno Pontecorvo, 3, I-56127 Pisa, Italy*
[4]*INFN, Laboratori Nazionali di Legnaro, Viale dell'Università 2, I-35020 Legnaro, Italy*

(Received 21 June 2015; accepted 22 October 2015; published online 9 November 2015)

We report on a scheme for particle detection based on the infrared quantum counter concept. Its operation consists of a two-step excitation process of a four level system, which can be realized in rare earth-doped crystals when a cw pump laser is tuned to the transition from the second to the fourth level. The incident particle raises the atoms of the active material into a low lying, metastable energy state, triggering the absorption of the pump laser to a higher level. Following a rapid non-radiative decay to a fluorescent level, an optical signal is observed with a conventional detector. In order to demonstrate the feasibility of such a scheme, we have investigated the emission from the fluorescent level $^4S_{3/2}$ (540 nm band) in an Er^{3+}-doped YAG crystal pumped by a tunable titanium sapphire laser when it is irradiated with 60 keV electrons delivered by an electron gun. We have obtained a clear signature that this excitation increases the $^4I_{13/2}$ metastable level population that can efficiently be exploited to generate a detectable optical signal. © *2015 AIP Publishing LLC*. [http://dx.doi.org/10.1063/1.4935151]

There is a significant interest in the development of devices for the detection of low rate, low energy deposition events, both for the axionic dark matter (DM) searches[1] and for the study of the coherent neutrino-nucleon scattering.[2,3] The so-called "invisible axion" has mass constrained in the range of 1 μeV–10 meV, and its coupling with normal matter and radiation is very weak.[4] In neutrino coherent scattering, the recoil energy for the nuclei of the target material is in the tens-of-eV range, when MeV neutrinos and average mass nuclei are considered.[5]

A very low value of energy threshold (~0.5 keV) has been reported in 440 g-mass semiconductor detectors[6] aimed at light-mass DM investigations. Arrays of cryogenic bolometers[7,8] have been proposed for neutrino physics, because the highest sensitivities[9] are accomplished only when a few grams of material act as a target.

The mentioned requirements are addressed in the present work with an all-optical detection scheme based on the infrared quantum counter concept (IRQC), proposed by Bloembergen[10] as a way to extend photon detection to the 1–100 μm wavelength range. The incident infrared photon is upconverted in a material that exhibits a four energy level system with $E_2 > E_3 > E_1 > E_0$, as those determined in wide bandgap materials doped with trivalent rare-earth (RE) ions,[11] and kept under the action of a pump laser source resonant with transition $1 \rightarrow 2$. In analogy with the infrared quantum counter, detection of the particle is then accomplished through the fluorescence photons emitted in the transition $3 \rightarrow 1$, as shown in Fig. 1.

In contrast to narrow-band, selective detection of infrared photons, a particle that interacts in an optical material, gives rise to several phenomena, including energy transfer processes from the host to the RE ion, which can be viewed as wideband excitation for the present purposes. The complex chain of events whereby a particle loses its energy in a material has been systematically investigated for the development of state-of-the-art scintillators.[13–16] Attention has been paid to the transitions in the visible, UV, and near infrared in those studies. Here, we want to focus on the fraction of the particle energy that is translated in the excitation of the low energy metastable level 1 indicated in Fig. 1, which can take place both through the decay of higher levels and directly from the ground state. This is motivated by the assumption that the particle energy loss is a process in which it is much more probable to increase the population of low energy atomic levels than highest ones. Such reasoning is supported by three points:

(1) the inelastic scattering of free electrons off bounded electrons is a major process in particle energy loss and is described by the Bethe-Bloch formula that privileges *low energy transfer* events;[17]
(2) another dominant process is the thermalization of the secondary electrons produced in the interaction that takes place through optical *phonon scattering*;

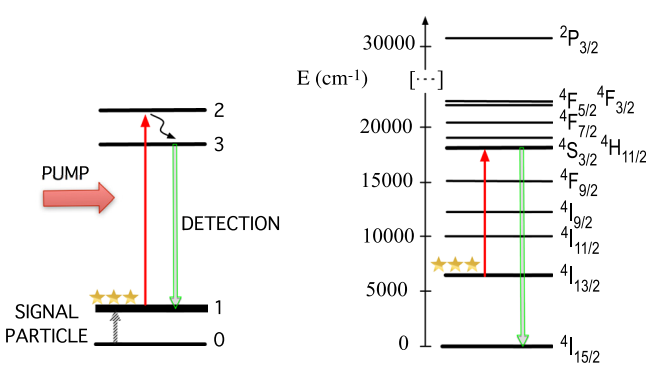

FIG. 1. *(Left)* Ideal four-level active material. *(Right)* Energy level scheme in YAG:Er, as derived from energy levels' values calculated in Ref. 12.

a)Electronic mail: Caterina.Braggio@unipd.it

(3) *infrared scintillation* in the range of 600–900 nm has been reported[16] with an intensity in excess of 10^5 photons per MeV. A light yield of $(79 \pm 8) \times 10^3$ has also been observed in YAG:(10%)Yb^{3+}, whose emission peaked around $\lambda = 1.03\ \mu m$.[18]

In view of these observations and provided the efficiency of the upconversion process is high,[19,20] the proposed scheme has the potential to generate a greater number of information carriers (photons) for a given energy release. In fact, the intrinsic threshold for particle detection coincides with E_1, which can be as low as a few tens of meV in proper materials, provided the crystal is cooled to a temperature such that the condition $E_1 \gg kT$ is satisfied. A cryogenically cooled crystal with $E_1 \sim 10$ meV would then allow extension of the upper limit in axion direct searches.[4] The measurements presented in this work are conducted at room temperature with a rare-earth doped material characterized by $E_1 = 0.74$ eV $(N_1/N_0 \sim 10^{-14})$. Another essential condition for achieving a detector threshold as low as E_1 when $E_1 \gg kT$ is that the extraction efficiency of the emitted fluorescence photons is highest. Such photons can in fact be lost because of total internal reflection or reabsorption, though the latter can be reduced in rare-earth doped materials by using high purity starting components in an ultra-clean environment.

The present work is organized as follows. We first investigate the response of a low concentrated YAG:(0.5%)Er^{3+} crystal to an electron gun excitation, which represents our particle signal in Fig. 1. These preliminary measurements include both the acquisition of cathodoluminescence (CL) spectra and the study of the $^4I_{13/2}$ metastable lifetime. We also estimate the efficiency of the laser-pumped YAG:Er crystal in the counting of photons delivered by a diode laser ($\lambda \approx 960$ nm). The core of the work is the study of the fluorescence stemming from the de-excitation of the $^4S_{3/2}$ level when the particle-excited crystal is continuously pumped by a laser resonant with the transition $^4I_{13/2} \rightarrow {}^4S_{3/2}$.

During the CL measurements of the YAG:Er crystal, a cylinder with diameter of 5 mm and height of 3 mm is mounted at the far end of the electron gun vacuum chamber that is enclosed inside a Pb-shielded cabinet.[21] The main transitions involved in the excitation process can be identified in the spectra shown in Fig. 2. The visible spectrum is obtained with a CCD spectrometer (Ocean Optics mod. Red Tide 650), whereas the infrared portion of the spectrum, displayed in the inset, is studied with a Fourier transform interferometer (Bruker Equinox 55). The interferometer is equipped with an InGaAs photodiode, sensitive in the range of 0.8–1.7 μm. The two sharp emission lines observed in the visible are doublets peaking at 401.5 and 405.1 nm and at 470.9 and 474.0 nm. They are attributed to 4*f*–4*f* transitions of the Er^{3+} ions in the YAG host, respectively, to intermanifold transitions $^2P_{3/2} \rightarrow {}^4I_{13/2}$ and $^2P_{3/2} \rightarrow {}^4I_{11/2}$. These transitions indicate that the metastable level $^4I_{13/2}$ population is increased also by the decay of higher levels excited by electron impact.

As far as the 540 nm band luminescence is concerned, CL spectra in YAG:Er single crystalline films have been very recently reported, which show a larger emission[22] than

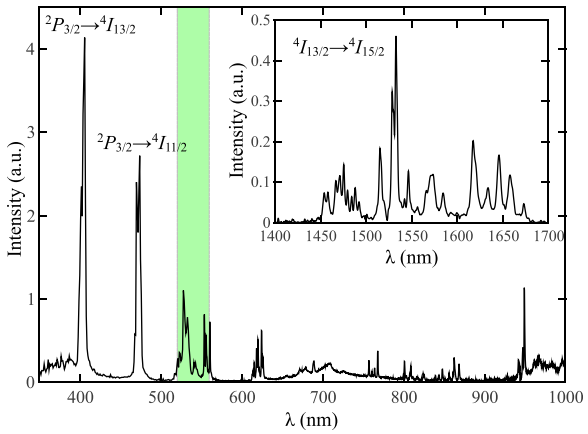

FIG. 2. CL spectra of YAG:Er. The results of Fourier transform interferometer (FT-IR) measurements are displayed in the inset.

in the present case. This might indicate that a portion of our 540 nm fluorescence band is absorbed in the 3 mm-thick crystal, where the electrons interaction region is limited to a few hundred μm (Ref. 23) from the surface, while the light detection is accomplished on the opposite crystal face.

In the inset, we show the infrared spectrum originating from the decay of the $^4I_{13/2}$ metastable level. This manifold around 1.53 μm is widely used for IR lasing.[24] The lifetime of this level is several milliseconds long and weakly depends on the crystal preparation and excitation source. Therefore, we have recorded, as shown in Fig. 3, the time evolution of the fluorescence emitted by the crystal excited with a 2.5 ms-duration electron pulse. The crystal response has been numerically computed by solving a first order kinetic equation for the population of the level excited by the current pulse shown in the figure. We obtain a lifetime value $\tau = 7.19 \pm 0.02$ ms, in a fair agreement with the literature data[25–27] obtained for optical excitation.

To study the IRQC efficiency, we have used as infrared source, a 960 nm wavelength diode laser. Upconversion is accomplished by pumping the $^4I_{13/2} \rightarrow {}^4S_{3/2}$ transition with a tunable Ti:Al_2O_3 laser. In Fig. 4, the fluorescence spectrum, obtained with a CCD spectrometer (Ocean Optics mod. Red), around 540 nm is reported. We estimate that the IRQC efficiency is of the order of 10^{-4} with a pump flux of

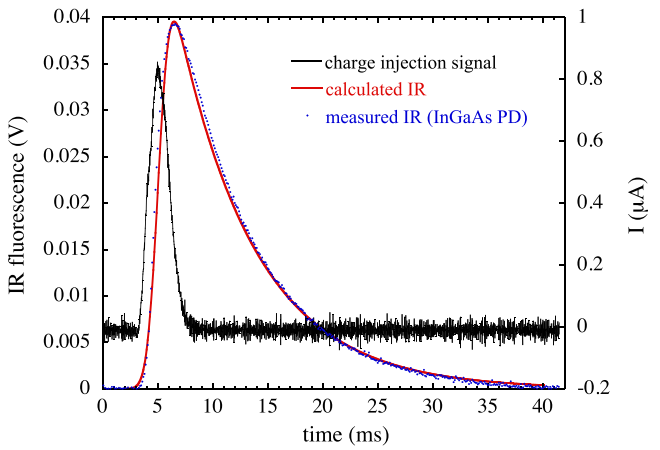

FIG. 3. Electron current waveform (right scale) and the 1.53 μm fluorescence signal (left scale) detected by an InGaAs photodiode with input bandpass filter centered at $\lambda = 1.490 \pm 0.25\ \mu m$.

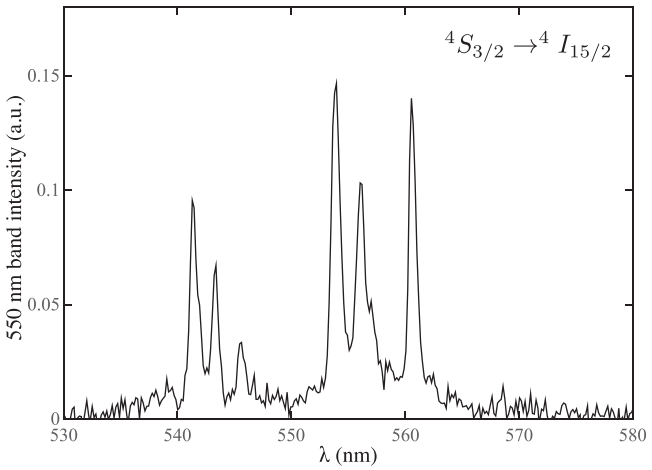

FIG. 4. 540 nm fluorescence spectrum originating from the double resonance with a laser diode at wavelength of 960 nm and a Ti:Al_2O_3 laser.

the order of 10 W/cm^2. Such a low efficiency is related to the properties of the host material, as reported in Ref. 28.

The experimental apparatus depicted in Fig. 5 was designed to test the particle detection through the IRQC scheme. A few hundred nA continuous current of 60 keV electrons impinges on the YAG:Er crystal, while a Ti:Al_2O_3 laser pumped the transition $^4I_{13/2} \rightarrow {}^4S_{3/2}$ as shown in the energy level scheme in Fig. 1. Pump light was allowed to impinge on the crystal by means of a 1.6 mm diameter multimode fiber. Detection of the fluorescence for the different laser pump wavelengths is accomplished by means of a lock-in amplifier connected to the output of a photomultiplier tube (PMT) and modulation of the intensity of the pump laser. A bandpass filter allows the PMT to collect the total intensity emitted only in the range of 540–560 nm.

In Fig. 6, the $^4S_{3/2}$ fluorescence intensity is plotted for different wavelengths of the pump laser. The measurement is repeated in the same conditions with the electron gun switched off in order to quantify the contribution of the double resonance with the pump laser only. The interaction of the electrons in the YAG:Er crystal can be discerned due to a

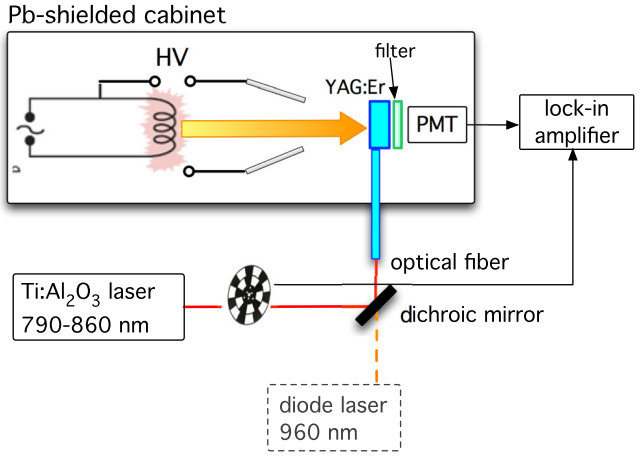

FIG. 5. Scheme of the experimental apparatus for particle detection. The output of a tunable Ti:Al_2O_3 laser is sent through a fiber to pump an YAG:Er crystal irradiated by ~60 keV electrons. In the preliminary measurements, radiation at a wavelength of $\lambda = 960$ nm is coupled to the crystal together with the pump radiation in order to study the 540 nm fluorescence band.

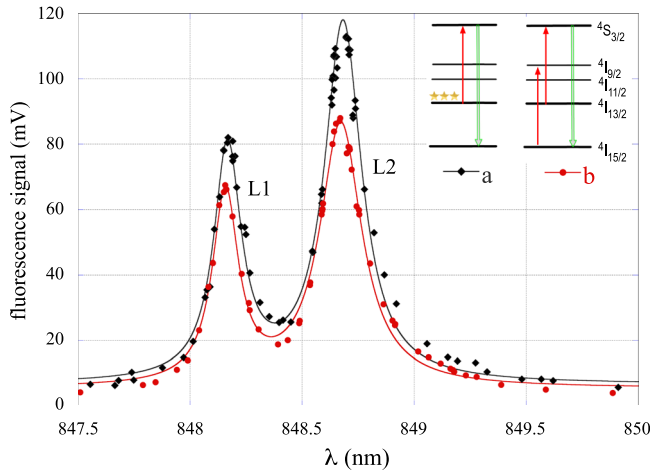

FIG. 6. Demonstration of the detector based on the IRQC concept: the 540 nm band fluorescence signal versus pump laser wavelength is greater when the electron gun excites the crystal (a) compared to the pump laser double resonance (b). L1 and L2 are transitions between sublevels in the $^4I_{13/2}$ and the $^4S_{3/2}$ manifolds.

30% increase of the areas under the Lorentzian curves. It is worth noticing that the contribution to the overall fluorescence due to the electrons excitation is geometrically unfavorable compared to the laser double resonance because of the electron short range in the crystal and of the crystal absorption. Results of the double Lorentzian fit of the data are shown in Table I. As we apply lock-in techniques through a modulation of the pump signal, it is straightforward that no signal above the PMT threshold is detected when the electron gun is on. The two lines correspond to two well defined transitions[11] between sublevels in the $^4I_{13/2}$ and the $^4S_{3/2}$ manifolds. We have also checked that the fluorescence signal depends linearly on the electron gun current in a range of 0.1–1.6 μA, as shown in Fig. 7(a). It is linear with the pump as well (Fig. 7(b)), as observed up to the maximum available light intensity (~280 mW).

In conclusion, a particle detector based on laser-driven, fluorescence emitting transitions in crystals has been outlined. We have shown that the IRQC scheme can be applied to the detection of particles through investigation of the fluorescence signal emitted by a laser-pumped Er^{3+}-doped crystal, whose intensity is proportional to the energy deposited in the crystal by the incident particles. The results have been obtained in YAG:Er, a crystal that for our purposes cannot be considered as ideal. The optimum crystal is preferably transparent to the pump until a particle interacts in the activated material and deposits its energy in the volume shined by the pump laser. This is not the present case, as shown in Fig. 6, where a significant fraction of the fluorescence is determined by the double resonance with the pump laser.

TABLE I. Results of the Lorentzian fit. w and a are the width of the peaks and their area, respectively.

		λ_{max}	w	a
L1	Pump	848.16 ± 0.01	0.14 ± 0.01	12.8 ± 0.8
	Pump + e^- gun	848.17 ± 0.02	0.15 ± 0.01	16.5 ± 1.1
L2	Pump	848.67 ± 0.01	0.23 ± 0.01	28.8 ± 1.1
	Pump + e^- gun	848.68 ± 0.01	0.2 ± 0.01	34.8 ± 1.1

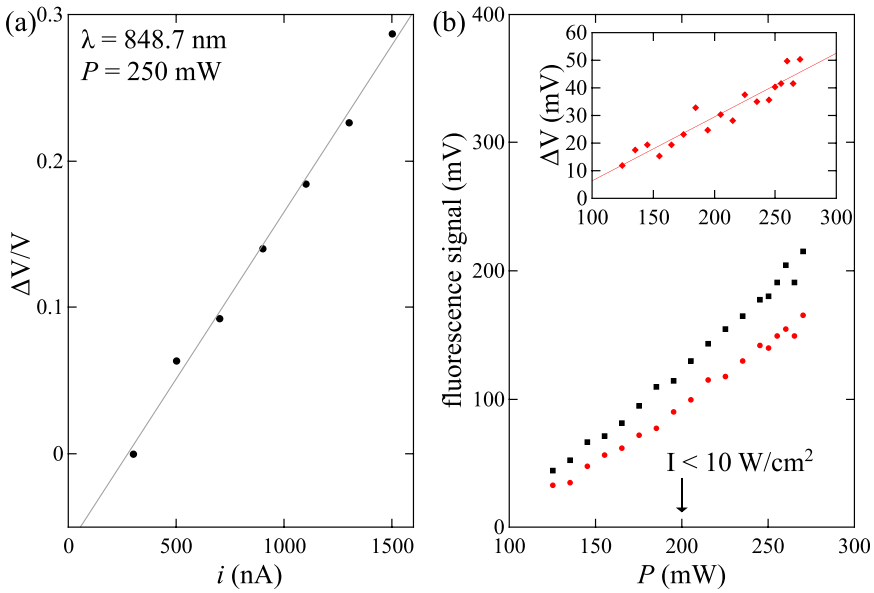

FIG. 7. (a) Relative increase of the 540 nm band intensity $\Delta V/V$ is linearly dependent on the current measured at the beam stopper. (b) Linear dependence of the fluorescence on the pump power P. The filled dot symbol is used for the data of the double resonance with the pump laser only, the filled squares represent the combination of the electron gun and the pump laser. An upper value of the estimated pump intensity at 200 mW is also displayed for reference.

Moreover, the host crystal (YAG) gives a much weaker IRQC output than in fluoride or tungstate hosts.[28] Another key requirement is the lifetime of the metastable level, and materials characterized by a much longer τ have been recently investigated, such as neodymium doped potassium lead bromide (KPb_2Br_5:Nd), in which $\tau = 57$ ms at 15 K.[29] This material presents another interesting aspect, because of its fluorescence at 1064 nm that decays to the metastable level $^4I_{11/2}$, offering the possibility to exploit looping cycles to increase the detection sensitivity.[30]

Improved IRQC efficiencies have been demonstrated when the crystal is cooled to liquid helium temperature, thanks to the sharpening of the involved atomic transitions.[28] This issue is worth investigation also in the present case, in which the first step of the double resonance process is due to the particle energy deposited in the crystal rather than to photon absorption.

The feasibility of the previously mentioned neutrino or axion experiments, to be performed in underground laboratories, also depends on the intrinsic radioactive background. We wish to point out the possibility of using the matrix isolation technique[31] to engineer a radio-pure material for experiments in which very low thresholds are required. Searches for dark matter axions based on kilogram-sized samples have been proposed,[1] and in neutrino investigations the required masses are even bigger (several kg), even so the manufacture of large samples is not a critical issue in matrix isolation.[32] Commercial cw lasers are available whose output power (W/cm^2) shall allow efficient upconversion,[19] indeed it is worth mentioning here that a scheme based on a multi-pass cavity might be exploited to use less pump power.

[1]P. Sikivie, Phys. Rev. Lett. **113**, 201301 (2014).
[2]D. Z. Freedman, Phys. Rev. D **9**, 1389–1392 (1974).
[3]A. C. Dodd, E. Papageorgiu, and S. Ranfone, Phys. Lett. B **266**, 434–438 (1991).
[4]*Axions: Theory, Cosmology, and Experimental Searches*, edited by M. Kuster, G. Raffelt, and B. Beltrán (Springer, 2008).
[5]A. Drukier and L. Stodolsky, Phys. Rev. D **30**, 2295–2309 (1984).
[6]C. E. Aalseth, P. S. Barbeau, N. S. Bowden, B. Cabrera-Palmer, J. Colaresi, J. I. Collar, S. Dazeley, P. de Lurgio, J. E. Fast, N. Fields, C. H. Greenberg, T. W. Hossbach, M. E. Keillor, J. D. Kephart, M. G. Marino, H. S. Miley, M. L. Miller, J. L. Orrell, D. C. Radford, D. Reyna, O. Tench, T. D. Van Wechel, J. F. Wilkerson, and K. M. Yocum, Phys. Rev. Lett. **106**, 131301 (2011).
[7]B. Cabrera, L. M. Krauss, and F. Wilczek, "Bolometric detection of neutrinos," Phys. Rev. Lett. **55**, 25–28 (1985).
[8]J. A. Formaggio, E. Figueroa-Feliciano, and A. J. Anderson, Phys. Rev. D **85**, 013009 (2012).
[9]C. Enss, *Cryogenic Particle Detection* (Springer-Verlag, Berlin, Heidelberg, 2005).
[10]N. Bloembergen, Phys. Rev. Lett. **2**, 84 (1959).
[11]A. K. Kaminskii, *Laser Crystals* (Springer-Verlag, Berlin, 1981).
[12]J. B. Gruber, J. R. Quagliano, M. F. Reid, F. S. Richardson, M. E. Hills, M. D. Seltzer, S. B. Stevens, C. A. Morrison, and T. H. Allik, Phys. Rev. B **48**, 15561–15573 (1993).
[13]P. A. Rodnyi, *Physical Processes in inorganic scintillators* (CRC Press LLC, 1997).
[14]M. J. Weber, J. Lumin. **100**, 35–45 (2002).
[15]W. Drozdowski, P. Dorenbos, J. de Haas, R. Drozdowska, A. Owens, K. Kamada, K. Tsutsumi, Y. Usuki, T. Yanagida, and A. Yoshikawa, IEEE Trans. Nucl. Sci. **55**, 2420–2424 (2008).
[16]W. Moses, M. Weber, S. Derenzo, D. Perry, P. Berdahl, and L. Boatner, IEEE Trans. Nucl. Sci. **45**, 462–466 (1998).
[17]G. F. Knoll, *Radiation Detection and Measurement* (Wiley, New York, 2010).
[18]P. Antonini, S. Belogurov, G. Bressi, G. Carugno, and D. Iannuzzi, Nucl. Instrum. Methods Phys. Res., Sect. A **486**, 799–802 (2002).
[19]W. F. Krupke, IEEE J. Quantum Electron. **20**, 20–28 (1965).
[20]J. C. Wright, D. J. Zalucha, H. V. Lauer, D. E. Cox, and F. K. Fong, J. Appl. Phys. **44**, 781 (1973).
[21]L. Barcellan, E. Berto, G. Carugno, G. Galet, G. Galeazzi, and A. F. Borghesani, Rev. Sci. Instrum. **82**, 95103 (2011).
[22]Y. Zorenko, V. Gorbenko, T. Zorenko, V. Savchyn, M. Batentschuk, A. Osvet, and C. Brabec, J. Lumin. **154**, 198–203 (2014).
[23]See physics.nist.gov/PhysRevData/Star/Text/method.html for calculation of the electrons' range.
[24]M. Eichhorn, S. T. Fredrich-Thornton, E. Heumann, and G. Huber, Appl. Phys. B **91**, 249 (2008).
[25]S. Payne, L. Chase, L. K. Smith, W. L. Kway, and W. F. Krupke, IEEE J. Quantum Electron. **28**, 2619–2630 (1992).
[26]N. Ter-Gabrielyan, M. Dubinskii, G. A. Newburgh, A. Michael, and L. D. Merkle, Opt. Express **17**, 7159 (2009).
[27]O. Toma and S. Georgescu, IEEE J. Quantum Electron. **42**, 192 (2006).
[28]L. Esterowitz, J. N. A. Schnitzler, and J. Bahler, Appl. Opt. **7**, 2053 (1968).
[29]E. Brown, C. B. Hanley, U. Hömmerich, A. G. Bluiett, and S. B. Trivedi, J. Lumin. **133**, 244–248 (2013).
[30]F. Auzel, Chem. Rev. **104**, 139–173 (2004).
[31]I. R. Dunkin, *Matrix-Isolation Techniques: A Practical Approach* (Oxford University Press, 1998).
[32]C. Pryor and F. Wilczek, Phys. Lett. B **194**, 137–140 (1987).